Universitat Politècnica de Catalunya (UPC)
Universitat Autònoma de Barcelona (UAB)
Universitat de Barcelona (UB)
Institut de Ciències Fotòniques (ICFO)

http://www.photonicsbcn.eu

Master in Photonics

MASTER THESIS WORK

TOWARDS INTERFEROMETRY WITH MATTER WAVE BRIGHT SOLITONS

Juan Polo Gomez

Supervised by Dr. Verònica Ahufinger Breto (UAB)

Presented on date 4th of September, 2012

Registered at

Escola Tècnica Superior d'Enginyeria de Telecomunicació de Barcelona

Towards interferometry with matter wave bright solitons

Juan Polo Gomez

Grup d'Òptica, Dept. de Física, Universitat Autònoma de Barcelona, E-08193 Bellaterra, Spain

E-mail: zestzestzest@gmail.com

Abstract. We study the implementation of a matter wave bright soliton interferometer formed by a Gaussian potential barrier placed at the center of a harmonic trap potential. After numerically evaluating the transmission coefficient of the potential barrier as a function of the ratio between the kinetic energy of an incident matter wave bright soliton and the height of the barrier, we focus on the case for which the transmitted and the reflected split solitons have the same number of atoms. This beam splitter behavior is fully characterized in terms of the phase and the energies of the two outcome solitons. The recombination process through the barrier is also investigated in terms of the phase difference between the two arms of the interferometer.

Keywords: matter wave solitons, interaction with potential barriers, atom interferometer.

1. Introduction

Interferometry has been for many years an important scientific tool with a myriad of applications, ranging from precision measurements to fundamental studies. Atomic interferometers that exploit the wave character of atoms allow for very high sensitivities due to the associated small wavelength. Moreover, the inherent atomic properties like mass or polarizability offer new possibilities for high-precision measurements of, for instance, fundamental constants, internal forces or rotations [1–4]. Specifically, the use of ultracold atoms, that can be precisely manipulated at the quantum level and can be held for long times in traps [5], provides very high precision and sensitivity [6]. Nevertheless, in linear interferometry, the minimum uncertainty in determining the phase difference is given by the standard quantum limit [7], i.e., the expected for a classical measurement. It has been shown that this limit can be surpassed, approaching the Heisenberg limit, using nonclassical input states [8–12] or entangled states within the interferometer in the regime of large atom number with controlled interactions [7]. One potential problem that atomic interferometers face is based on the fact that the wavefunction disperses during its evolution. A possible solution is to use matter wave bright solitons in Bose-Einstein condensates (BEC). Matter wave bright solitons are

solitary waves with attractive interatomic interactions, that prove to be rather robust when colliding with each other or when interacting in an external potential and present a very important characteristic: they can propagate without dispersion [13, 14]. Within the mean field approximation, their dynamics is well described by the Gross Pitaevskii equation (GPE), although effective particle models also exist and have been used to characterize the center of mass trajectories of the solitons [15–17]. Note that the use of solitons for interferometry [18–26] opens new perspectives and allows to address fundamental questions due to the dual nature (particle and wave) of solitons in BEC. Within the quasi 1-D limit, collisions of matter wave bright solitons with barriers have been largely studied in order to coherently split the soliton [25] and the recombination of identical solitons through a potential barrier has also been addressed [19, 20].
In this work, we will investigate the implementation of a full matter wave bright soliton interferometer formed by a harmonic potential trap and a Gaussian barrier at its center in which the incident matter wave soliton splits and the two output split ones recombine after some time. This setup is currently under experimental study in the group of Prof. R. Hulet [27]. In section 2, we introduce the physical system that we are considering. In section 3, we analyze in detail the role of the barrier as a beam splitter characterizing the two output solitons as a function of the system parameters. Section 4 is devoted to the recombination process and in section 5 we present the conclusions.

2. Physical system

We consider a Bose-Einstein condensate of ^{7}Li at $T = 0$ whose dynamics within the mean field approach is described by the 3D time dependent GPE [28]:

$$i\hbar\frac{\partial}{\partial t}\varphi(\mathbf{r},t) = \left(-\frac{\hbar^2\nabla^2}{2m} + V(\mathbf{r}) + g_{3D}|\varphi(\mathbf{r},t)|^2\right)\varphi(\mathbf{r},t)\ ; \tag{1}$$

where the first term of the right hand side of Eq. (1) corresponds to the kinetic contribution, the second term is the external potential that reads $V(\mathbf{r}) = m[\omega_r^2(x^2 + y^2) + \omega_z^2 z^2]/2$, and the last term is the nonlinear term, where $g_{3D} = 4\pi\hbar^2 a_s N/m$, and N, a_s and m are the atom number, s-wave scattering length and atomic mass, respectively. The wavefunction is normalized to 1, and the scattering length is negative, $a_s < 0$, which means that the interactions are attractive. For sufficiently tight radial confinement ($\omega_r \gg \omega_z$), but allowing that interactions remain 3D, $a_s \ll (\hbar/m\omega_r)^{1/2}$, it is possible to separate the radial and the axial dynamics using the ansatz $\varphi(\mathbf{r}) = \Psi(z)(m\omega_r/\pi\hbar)^{1/2}\exp(-m\omega_r[x^2+y^2]/2\hbar)$, obtaining the reduced 1D GPE [26]:

$$i\hbar\frac{\partial}{\partial t}\Psi(z,t) = \left(-\frac{\hbar^2}{2m}\frac{\partial^2}{\partial z^2} + V(z) + g_{1D}|\Psi(z,t)|^2\right)\Psi(z,t), \tag{2}$$

where $g_{1D} = 2N\hbar\omega_r a_s$ [29] and the external potential reduces to $V(z) = \frac{1}{2}m\omega_z^2 z^2$. By using Crank-Nicolson method in imaginary time evolution we calculate the ground state of the system for state of the art parameter values [13]: $\omega_r = 2\pi \times 710$ Hz, $\omega_z = 2\pi \times 78$ Hz, $a_s = -0.21$ nm, $m = 1.165 \times 10^{-26}$ kg and $N = 15000$ atoms, obtaining a matter

wave bright soliton.

Once a stable soliton is created, we displace the center of the harmonic potential a distance z_0 and introduce a Gaussian potential barrier centered at $z = 0$ on which the soliton will collide. The external potential reads now:

$$V(z) = \frac{1}{2}m\omega_z^2(z - z_0)^2 + V_b e^{\frac{z^2}{2\sigma^2}}, \tag{3}$$

where V_b and σ are the strength and the width of the barrier, respectively. With this configuration we implement an interferometer for matter wave bright solitons that can be separated into three steps: a) the soliton is split in two by colliding with the barrier; b) the two split solitons evolve in the external harmonic potential reducing their kinetic energy and increasing the potential one until they stop and go back in opposite directions; and c) a recollision of the solitons with the barrier occurs at the center of the trap. Fig. 1 shows the process schematically.

In order to characterize the dynamics of the splitting of the initial soliton and the

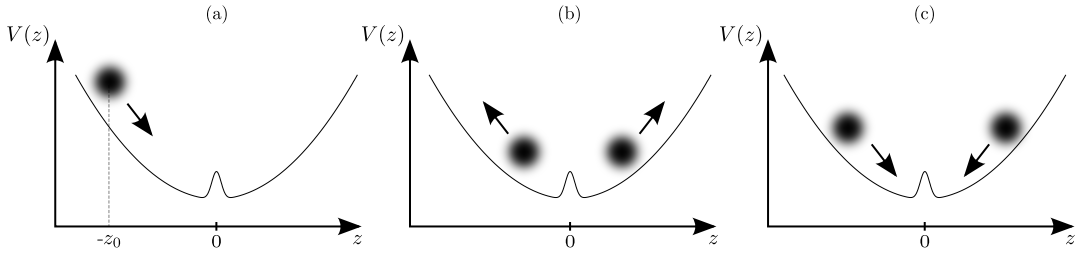

Figure 1. Schematics of the interferometer sequence: (a) initial situation in which the soliton is displaced with respect to the center of the harmonic potential trap by a distance z_0; (b) the two split solitons obtained after the collision with the barrier separate from each other (c) the two solitons return to the position of the barrier and recollide.

evolution of the system afterwards, we calculate the expected value of the position and momentum for the soliton before its collision with the barrier and for the two solitons obtained after the splitting:

$$\langle z_i \rangle = K_i^{-1} \int_{C_i} dz |\Psi(z,t)|^2 z, \tag{4}$$

$$\langle p_i \rangle = -i\hbar K_i^{-1} \int_{C_i} dz \Psi^*(z,t) \frac{\partial}{\partial z} \Psi(z,t), \tag{5}$$

where $K_i = \int_{C_i} dz |\Psi(z,t)|^2$ and C_i denotes the region containing the solitons: being $i = I, R, T$ for Incident, Reflected and Transmitted regions, respectively. We also define the position and momentum uncertainty:

$$\Delta z_i = (\langle z_i^2 \rangle - \langle z_i \rangle^2)^{1/2}, \tag{6}$$

$$\Delta p_i = (\langle p_i^2 \rangle - \langle p_i \rangle^2)^{1/2}, \tag{7}$$

where:

$$\langle z_i^2 \rangle = K_i^{-1} \int_{C_i} dz |\Psi(z,t)|^2 z^2, \tag{8}$$

$$\langle p_i^2 \rangle = -\hbar^2 K_i^{-1} \int_{C_i} dz \Psi^*(z,t) \frac{\partial^2}{\partial z^2} \Psi(z,t). \quad (9)$$

The number of particles of each soliton is given by $N_i = NK_i$ and the energy per particle reads:

$$e_i = \frac{E_i}{N} = \int_{C_i} dz \left[\frac{\hbar^2}{2m} \left| \frac{\partial}{\partial z} \Psi(z,t) \right|^2 + V(z)|\Psi(z,t)|^2 + g_{1D}|\Psi(z,t)|^4 \right], \quad (10)$$

where the first term of the right hand side corresponds to the kinetic energy E_k, the second one is the external potential energy, E_{ho}, and the last one is the internal energy due to the atom-atom interaction, E_{int}. Note also that by direct integration of the GPE under the stationary ansatz $\Psi(z,t) = \Psi(z) \exp(-i\mu t/\hbar)$, where μ is the chemical potential, we obtain $\mu = E_k + E_{ho} + 2E_{int}$ [28].

3. Splitting process

In this section we analyze the main aspects that affect the dynamics of the splitting process of a matter wave bright soliton under the collision with a Gaussian potential barrier.

3.1. Transmission

By an instantaneous displacement of the trapping potential, the center of the soliton is placed at $-z_0$ and the soliton acquires a potential energy that, as predicted by particle models [30, 31], is fully converted into kinetic energy once the soliton reaches the center of the potential. Therefore, the kinetic energy of the soliton when interacting with the barrier is $E_{ho} = \frac{1}{2} m\omega_z^2 (z - z_0)^2$. We have checked that this result is in full agreement with Eq. (10).

Fig. 2(a) shows the numerically evaluated transmission coefficient as a function of the ratio between the kinetic energy of the soliton and the height of the potential barrier for a fixed potential barrier height of $V_b = 17.14\hbar\omega_z$ (squares), and for a fixed kinetic energy of $E_k = 10.83\hbar\omega_z$ (circles); in both cases $\sigma = 0.5$ μm. The different behaviors obtained close to $T = 1$ can be understood by taking into account that the changes in the strength of the potential or in the kinetic energy of the incident soliton do not produce exactly the same effect due to the different area that the soliton has to penetrate in order to pass through the barrier. Nevertheless, a common feature is the high slope in the region where the transmission coefficient is 0.5, i.e. where the initial soliton splits into two solitons with the same number of atoms, which makes this point very sensitive to the initial conditions. Fig. 2(b) shows the transmission as a function of the width of the barrier (circles) for a fixed ratio $E_k/V_b = 0.63$. As expected, the increase of the width of the barrier corresponds to a decrease in transmission. In Fig. 2, we also plot the analytical transmission coefficient for a rectangular barrier (dotted-dashed line), which

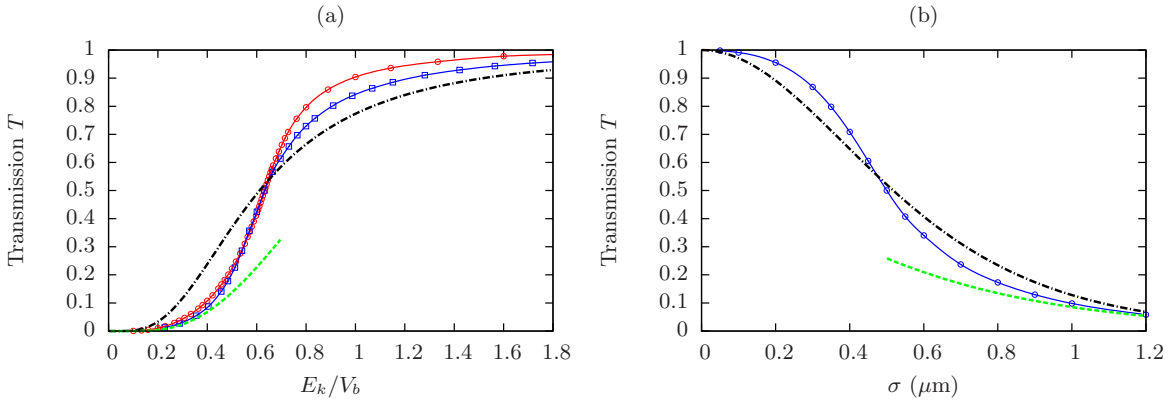

Figure 2. Transmission as a function of (a) the ratio between E_k/V_b and (b) the width of the barrier obtained by fixing $E_k = 17.14\hbar\omega_z$ (circles) or $V_b = 10.83\hbar\omega_z$ (squares). The analytic result for a rectangular barrier (dotted-dashed line) and for the WKB approximation (dashed line) in the linear case are also plotted. The parameters of the system are $N = 15000$, $\omega_z = 2\pi \times 78$ Hz, $\omega_r = 2\pi \times 710$ Hz, $a_s = -0.21$ nm. In (a), $\sigma = 0.5$ μm and in (b) $E_k/V_b = 0.63$.

reads [32]:

$$T_{\sqcap_{E<V_b}} = \frac{1}{1 + \frac{V_b^2 \sinh^2(k_1(2\sigma))}{4E(V_b - E)}} \qquad T_{\sqcap_{E>V_b}} = \frac{1}{1 + \frac{V_b^2 \sin^2(k_1(2\sigma))}{4E(E - V_b)}} \; ; \tag{11}$$

where $k_1 = \sqrt{2m|V_b - E_k|/\hbar^2}$; and the Wentzel–Kramers–Brillouin (WKB) approximation (dashed line). The WKB approximation estimates the transmission coefficient, for small values of T and for potentials that do not change abruptly, taking into account the shape of the potential and considering the fact that the amplitude and the phase of the wave function vary slowly. The detailed analytical derivation of the transmission coefficient can be found in [32]:

$$T_{\mathrm{WKB}} \simeq \left(e^{\frac{1}{\hbar}\int_a^b dz\sqrt{2m(V(z)-E_k)}} + \frac{1}{4} e^{\frac{-1}{\hbar}\int_a^b dz\sqrt{2m(V(z)-E_k)}} \right)^{-2} \; ; \tag{12}$$

where a and b are the z-axis points where the kinetic energy and the barrier coincide, which for the Gaussian shape barrier are $b = -a = \sqrt{2\sigma^2 \ln(V_b/E_k)}$.

Note that these analytical transmission functions (Eq. (11) and (12)) are only valid in the linear regime. Therefore, in order to be valid for our numerical simulation E_k has to be large enough or the width of the barrier small enough to minimize the interaction time of the soliton with the barrier. Nevertheless, our specific setup limits these two parameters: the minimum width of the barrier is fixed by the diffraction limit, since the Gaussian potential is experimentally created by using a focalized laser beam with a beam waist equal to σ and the kinetic energy is limited by the finite potential trap displacement, z_0.

Moreover, there is an additional aspect that makes the comparison with the analytical functions difficult: the soliton is a wave packet described by a macroscopic wavefunction, whereas the analytical cases consider plane waves. Therefore, while plane waves have a

well defined momentum, the soliton has a very well defined position and the momentum uncertainty is very large, fulfilling the uncertainty relation $\Delta x_I \Delta p_I \geq \hbar/2$ close to the saturation value. For instance, for an incident soliton with $N = 15000$ the uncertainties using Eq. (6) and (7) are $\Delta x_I = 0.583$ nm and $\Delta p_I/\hbar = 0.898$ 1/nm, giving $\Delta x_I \Delta p_I/\hbar = 0.524$.

In spite of the discussed limitations, the rectangular potential barrier fits rather well with the numerical results (see Fig. 2). However the slope of the transmission function for the rectangular barrier near $T = 0.5$, region of interest for interferometric applications, is lower than the one obtained numerically with the Gaussian barrier. The WKB approximation agrees with the numerical transmission coefficient when $T \to 0$. However this region is out of the regime of interferometric applications where the aim is to split the soliton in two identical solitons ($T = 0.5$).

Fig. 3 shows the potential strength V_b as a function of E_k for which $T = 0.5$ and for two different values of the number of particles N. We can observe that the dependence is approximately linear and independent of N for large kinetic energies. Nevertheless, for small kinetic energies the nonlinearity starts to play an important role and breaks the linear dependence (see inset of Fig. 3). In the following we consider a soliton with $N = 15000$. This value has been chosen in order to obtain two solitons in the splitting process i.e, the nonlinearity is sufficient to compensate the dispersion after the splitting, where the number of atoms of each of the outcome solitons is $N/2$.

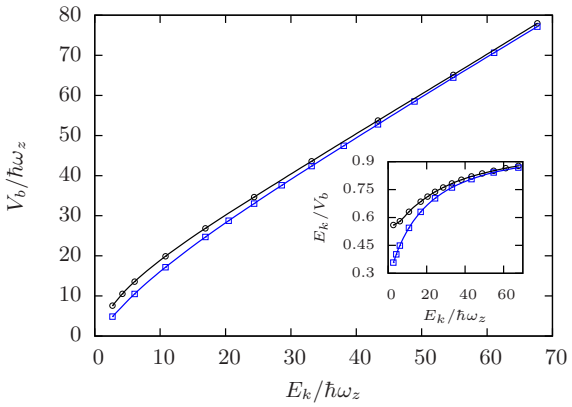

Figure 3. Potential barrier height as a function of the kinetic energy of the incident soliton for a fixed transmission coefficient $T = 0.5$, for an incident soliton of $N = 15000$ (squares) and $N = 7500$ (circles). The inset shows the ratio E_k/V_b as a function of the kinetic energy. The rest of the parameters of the system are $\omega_z = 2\pi \times 78$ Hz, $\omega_r = 2\pi \times 710$ Hz, $a_s = -0.21$ nm and $\sigma = 0.5$ μm.

3.2. Energy and Phase

The sensitivity of an interferometer has a strong dependence on how the phase difference is measured and for how long the split paths can accumulate phase without losing coherence [6]. Therefore, in section 4, we will analyze the phase evolution of the incident

soliton and of the two split solitons produced by the interaction with the barrier. Nevertheless, in this section we study first the phase difference between the transmitted and reflected solitons, introduced by the interaction with the barrier during the splitting process, by setting the harmonic external potential equal to zero. Fig. 4(a) shows

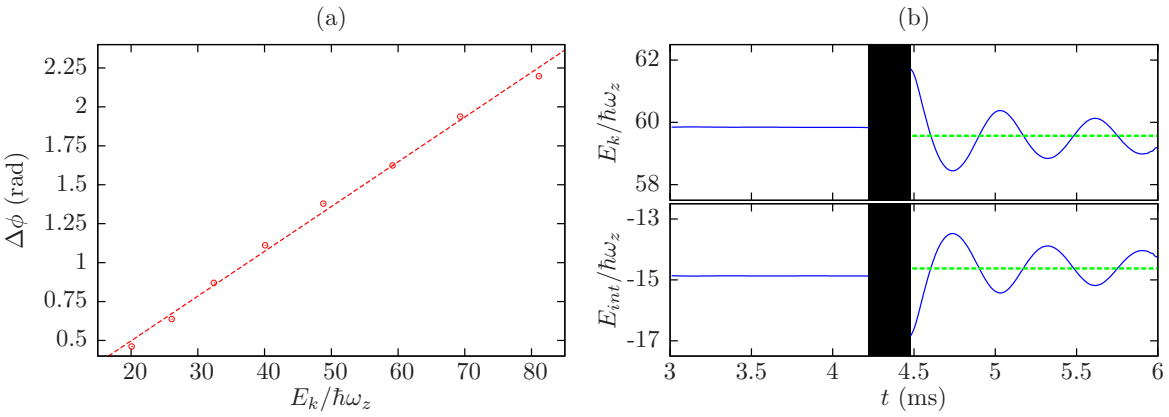

Figure 4. (a) Phase difference between the transmitted and the reflected soliton as a function of the kinetic energy of the incident soliton for $T = 0.5$. (b) Kinetic and internal energy for a total reflected soliton with initial kinetic energy $E_k = 58.85\hbar\omega_z$. The solid (dashed) line shows the time averaged energy before (after) the collision with the barrier for both E_k and E_{int}. The interval of time in which the collision with the barrier occurs is marked with the black region. The parameters used are: $N = 15000$, $\omega_r = 2\pi \times 710$ Hz, $\omega_z = 0$ Hz, $\sigma = 0.5$ μm and $a_s = -0.21$ nm.

the linear dependence of the phase difference between the transmitted and the reflected soliton, introduced by the reflection process, with the kinetic energy of the incident soliton. We consider $N = 15000$, potential width $\sigma = 0.5$ μm and a height such that the $T = 0.5$ condition is fulfilled, i.e., the two resulting solitons have the same number of atoms. By using expression (10), one can also calculate the evolution of the different contributions to the energy during the splitting process. We obtain that the reflected soliton has less kinetic energy than the transmitted one, and moreover, in the reflection process some kinetic energy is transfered to internal energy. Therefore, the transmitted and reflected solitons are not identical energetically. As an example, an incident soliton with an initial energy $E_k = 20.08\hbar\omega_z$ and $E_{int} = -14.84\hbar\omega_z$ splits into two solitons with the same number of particles when interacting with a barrier with $V_b = 20.57\hbar\omega$ and $\sigma = 0.5$ μm. The kinetic (internal) energy for the reflected and the transmitted soliton is $E_{k_T} = 5.20\hbar\omega_z$ ($E_{int_T} = -1.73\hbar\omega_z$) and $E_{k_R} = 3.57\hbar\omega_z$ ($E_{int_R} = -1.80\hbar\omega_z$), respectively. Although the total energy is conserved, $E_{k_R} + E_{int_R} + E_{k_T} + E_{int_T} = E_k + E_{int}$, it is clear that the reflected soliton has less energy than the transmitted one. An extreme case occurs for the total reflection of a soliton of $N = 15000$ where the transfer of kinetic to internal energy is clearly observed (Fig. 4(b)): the solid (dashed) line shows the time averaged energy before (after) the collision with the barrier for both E_k and E_{int}. It is worth noticing that the reflection process can also induce breathing excitations in which some fraction of the energy is exchanged periodically between E_k and E_{int} as shown in

Fig. 4(b), for the total reflection case ($T = 0$).

4. Recombination process

In this section we address the last step of the proposed implementation of a matter wave bright soliton interferometer, i.e., the free evolution of the split solitons and their recombination at the center of the harmonic potential (Fig. 1(c)). We consider the case described in section 3.2 in which one soliton collides with a Gaussian barrier and splits into two solitons with the same N and a relative phase induced by the potential barrier. During their evolution in the harmonic potential, the phases of the split solitons evolve differently due to the different velocity acquired during the splitting process (see section 3.2) as shown in Fig. 5. The incident soliton increases its phase as it propagates towards the barrier. After the collision with the barrier at $t = 4.34$ ms, two solitons appear with a phase difference (see inset Fig.5) as described in section 3.2. After their evolution in the harmonic potential performing a dipole oscillation, the two split solitons collide at the position of the barrier at $t = 10.40$ ms. The outcome of this collision depends on the relative phase between the two solitons that recombine. In general, one obtains two solitons with different number of particles after the recombination. Therefore, the accumulated relative phase in the two arms of the interferometer can be determined by measuring the relative particle number of the two outgoing solitons [25].

Fig. 6 shows different outputs of the studied atomic interferometer corresponding to

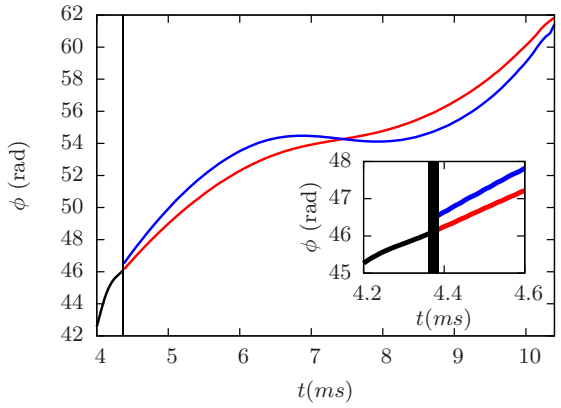

Figure 5. Time evolution of the phase of the incident soliton (black line) before the interaction with the barrier and of the reflected (blue line) and transmitted (red line) soliton created in the splitting process during its dipole oscillation in the harmonic trap. The parameters used are $N = 15000$, $\omega_z = 2\pi \times 78$ Hz, $\omega_r = 2\pi \times 710$ Hz, $a_s = -0.21$ nm, $E_k = 10.74\hbar\omega_z$, $\sigma = 0.5$ μm, the potential used for splitting into two solitons with the same number of particles is $V_b = 17.70\hbar\omega_z$. The time interval in which the collision with the barrier occurs is marked with the black region. The inset shows an enlarged view of the splitting process.

different phase differences between the recombined solitons. The phase difference in this

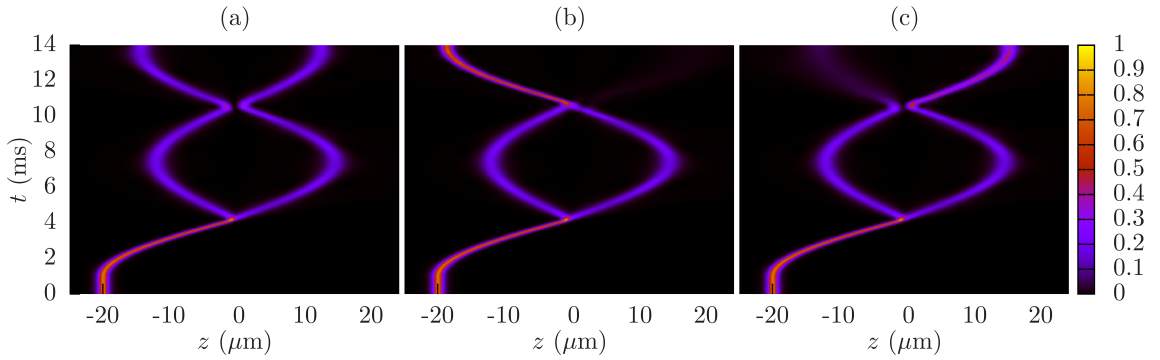

Figure 6. Recollison process for imprinted phases $\phi = 3.32$ rad (a), $\phi = 0$ rad (b), $\phi = 1.75$ rad (c), which produce 50% (50%), 95% (5%) and 25% (75%) of the initial number of particles at the left (right) output, respectively. The parameters used are $N = 15000$, $\omega_z = 2\pi \times 78$ Hz, $\omega_r = 2\pi \times 710$ Hz, $a_s = -0.21$ nm, $z_0 = -20$ μm, $\sigma = 0.5$ μm, $V_b = 17.70\hbar\omega_z$ for the splitting and $V_b = 20.44\hbar\omega_z$ in the recollision.

numerical experiment has been imposed by phase imprinting [33] in one of the arms of the interferometer i.e, $\Psi(z,t) \rightarrow \Psi(z,t)e^{i\phi}$. It is important to note that the Gaussian potential barrier used in the recombination process has been chosen in such a way that the transmission for each of the counterpropagating incident solitons is $T = 0.5$. Also, as seen in Fig. 6(c), when the number of particles of one of the two outputs is below the critical number for the stability of the soliton, the corresponding wavefunction disperses; this effect can be avoided by using incident solitons with a larger number of particles although it does not compromise the performance of the interferometer.

5. Conclusions

In this work we have studied the implementation of an atomic interferometer using matter wave bright solitons in a combined potential formed by a 1D harmonic potential and a Gaussian potential barrier in its center. We have calculated the transmission coefficient for the collision of an incident soliton with a Gaussian barrier and we have compared our numerical results with the analytical expression for a rectangular barrier and for the WKB approximation. Focusing on the case in which the transmission coefficient is 0.5, in order to obtain after the collision two solitons with the same number of particles, we have studied the splitting process in detail. We have found that the phase difference introduced during the splitting process presents a linear dependence with the kinetic energy of the incident soliton. Also, we have observed that one of the limiting effects in the splitting process is the different velocities acquired by the reflected and the transmitted solitons. This is due to the transfer of kinetic energy to internal energy that occurs in the reflection process. Another effect observed during the reflection process for high enough number of particles is the appearance of breathing excitations, which decay after a certain relaxation time. The recombination of the two split solitons is

also studied as a function of the phase difference in the two arms of the interferometer that determines the difference in atom number for the two outcome solitons after the recombination. Therefore, the studied system is a potential candidate for implementing atomic interferometry, due to the absence of dispersion of the matter wave function and the allowance for large coherent evolution times.

6. Acknowledgment

I would like to thank my supervisor Dr. Verònica Ahufinger for all her guidance and advise. I would also like to thank Albert Benseny, Daniel Viscor and Juan Luís Rubio for their comments and suggestions and Elena-Ruxandra Cojocaru for her support.

7. References

[1] A. D. Cronin, J. Schmiedmayer and D. E. Pritchard, Rev. Mod. Phys. **81**, 1051 (2009)
[2] M. Kasevich and S. Chu, Appl. Phys. B **54**, 321 (1992)
[3] T. L. Gustavson, P. Bouyer and M. A. Kasevich, Phys. Rev. Lett. **78**, 2046 (1997)
[4] J. B. Fixler *et al.*, Science **315**, 74 (2007)
[5] M. Gildemeister *et al.*, Phys. Rev. A **81**, 031402(R) (2010)
[6] J. Grond *et al.*, New J. Phys, **12** 065036 (2010)
[7] C. Gross *et al.*, Nature **464**, 1165 (2010)
[8] J. Hald *et al.*, Phys. Rev. Lett. **83**, 1319 (1999)
[9] A. Kuzmich, L. Mandel and N. P. Bigelow, Phys. Rev. Lett. **85**, 1594 (2000)
[10] V. Meyer *et al.*, Phys. Rev. Lett. **86**, 5870 (2001)
[11] D. Leibfried *et al.*, Science **304**, 1476 (2004)
[12] C. F. Roos *et al.*, Nature **443**, 316 (2006)
[13] L. Khaykovich *et al.*, Science **296**, 1290 (2002)
[14] K. E. Strecker, G. B. Partridge, A. G. Truscott R. G. Hulet, Nature **417**, 150 (2002)
[15] A. D. Martin, C. S. Adams, and S. A. Gardiner, Phys. Rev. A **77**, 013620 (2008)
[16] A. D. Martin, C. S. Adams, and S. A. Gardiner, Phys. Rev. Lett. **98**, 020402 (2007)
[17] D. Poletti *et al.*, Phys. Rev. Lett. **101**, 150403 (2008)
[18] A. I. Streltsov, O. E. Alon, and L. S. Cederbaum, Phys. Rev. Lett. **99**, 030402 (2007)
[19] J. L. Helm, T. P. Billam and S. A. Gardiner, Phys. Rev. A **85**, 053621 (2012)
[20] T. P. Billam, S. L. Cornish, and S. A. Gardiner, Phys. Rev. A **83**, 041602(R) (2011)
[21] S. L. Cornish *et al.*, Physica D **238**, 1299 (2009)
[22] C. Weiss and Y. Castin, Phys. Rev. Lett. **102**, 010403 (2009)
[23] A. I. Streltsov, O. E. Alon, and L. S. Cederbaum, Phys. Rev. A **80**, 043616 (2009)
[24] U. Al Khawaja and H. T. C. Stoof, New J. Phys. **13**, 085003 (2011)
[25] A. D. Martin and J. Ruostekoski, New J. Phys. **14**, 043040 (2012)
[26] T. P. Billam, S. A. Wrathmall, and S. A. Gardiner, Phys. Rev. A **85**, 013627 (2012)
[27] P. Dyke, S. Lei and R. Hulet, Book of Abstracts 23rd ICAP, Palaiseau, France, page 174 (2012)
[28] F. Dalfovo *et al.*, Rev. Mod. Phys. **71**, 463 (1999)
[29] L. Khaykovich, *et al.*, Science **296**, 1290 (2002)
[30] A. D. Martin, C. S. Adams, and S. A. Gardiner, Phys. Rev. Lett. **98**, 020402 (2007)
[31] R. Scharf and A. R. Bishop, Phys. Rev. A **46**, R2973 (1992)
[32] D. Bohm, Quantum theory, (Prentice-Hall, 1951)
[33] L. Dobrek *et al.*, Phys. Rev. A **60**, R3381 (1999)